Dissociation Kinetics of the Streptavidin-Biotin Interaction Measured using Direct Electrospray Ionization Mass Spectrometry Analysis

Lu Deng, Elena N. Kitova, and John S. Klassen*

Department of Chemistry and Alberta Glycomics Centre, University of Alberta, Edmonton, Alberta, Canada T6G 2G2

* Email: john.klassen@ualberta.ca

Abstract

Dissociation rate constants (k_{off}) for the model high affinity interaction between biotin (B) and the homotetramer of natural core streptavidin (S_4) were measured at pH 7 and temperatures ranging from 15 to 45 °C using electrospray ionization mass spectrometry (ESI-MS). Two different approaches to data analysis were employed, one based on the initial rate of dissociation of the (S_4 + 4B) complex, the other involving non-linear fitting of the time-dependent relative abundances of the (S_4 + *i*B) species. The two methods were found to yield k_{off} values that are in good agreement, within a factor of two. The Arrhenius parameters for the dissociation of the biotin-streptavidin interaction in solution were established from the k_{off} values determined by ESI-MS and compared to values measured using a radiolabeled biotin assay. Importantly, the dissociation activation energies determined by ESI-MS agree, within 1 kcal mol^{-1}, with the reported value. In addition to providing a quantitative measure of k_{off}, the results of the ESI-MS measurements revealed that the apparent cooperative distribution of (S_4 + *i*B) species observed at short reaction times is of kinetic origin and that sequential binding of B to S_4 occurs in a non-cooperative fashion with the four ligand binding sites being kinetically and thermodynamically equivalent and independent.

Introduction

Non-covalent interactions between proteins and between proteins with other biopolymers, small molecules or metal ions are critical to most cellular processes. The abundances of protein complexes and their lifetimes reflect the rates of the corresponding association and dissociation reactions. Quantification of the kinetic parameters - the association and dissociation rate constants (k_{on} and k_{off}, respectively) - under specific solution conditions (e.g. pH, temperature, ionic strength) is important in understanding the structure and function of protein complexes and is relevant to drug design [1-3]. There exist a number of established experimental techniques for measuring the rates of biochemical reactions, including association and dissociation reactions. These include surface plasmon resonance [4-5], spectroscopic methods (e.g., atomic force spectroscopy, circular dichroism or fluorescence-based approaches) [6-10], kinetic capillary electrophoresis [11-12], radiolabeling combined with filtration/dialysis [13-14] and NMR [15]. Many of these techniques require the labelling of one of the binding partners, their attachment to a surface or some other manipulation of the system, which can complicate the interpretation of the kinetic data and, in some instances, influence the rates of the reactions being investigated [16].

Electrospray ionization mass spectrometry (ESI-MS) has emerged as an important addition to the arsenal of techniques available for measuring the kinetics of chemical and biochemical reactions [17-28]. The ESI-MS approach is attractive as there is no requirement for labelling or immobilization since the identity of reactants and products and, possibly intermediates, can usually be established directly from the measured mass-to-charge ratios (m/z) [18,29]. Moreover, ESI-MS analysis allows for multiple reactions to be monitored simultaneously, a feature not associated with most kinetic assays. The determination of reaction rates by ESI-MS analysis

normally follows one of two general strategies: on-line (real-time) monitoring of the reaction mixture, and off-line analysis, usually following a quench step that stops the reaction. The advantage of the on-line approach is that it allows, in principle, for direct analysis of the time-dependent distribution of reactants, intermediates and products. The minimum acquisition time for an ESI mass spectrum, which is typically in the s - min range (although it varies between instruments and the nature of the sample being analyzed), places restrictions on the speed of reactions that can be reliably analyzed using the on-line approach. For this reason, real-time ESI-MS kinetic measurements are most commonly applied to relatively slow reactions, with timescales >min. However, there are examples where ESI-MS has been successfully applied to relatively fast reactions, in the ms – s range [17-18,20,22,24-25]. The measurement of fast kinetics typically requires the use of rapid mixing systems, such as a continuous-flow [17-18,20,22], rapid quenched-flow apparatus [24] or stopped-flow [25-26]. The off-line approach is generally easier to implement and affords greater flexibility in terms of the experimental conditions under which the reactions are carried out. For example, this approach is suitable for the analysis of enzyme kinetics under solution conditions that are not amenable to direct ESI-MS analysis, such as high concentrations of salts or non-volatile buffers (e.g. PBS, citrate, HEPES or TRIS) that are commonly used to stabilize proteins and ensure relevance to physiological conditions. Following the quench step, the solvent composition can be altered in order to facilitate detection of reactants or products by ESI-MS. However, a limitation of the off-line approach is that information on the distribution of species present under the reaction conditions of interest may be lost.

ESI-MS has been used to study the reaction rates for a variety of non-covalent protein interactions, including protein-protein [19-20,30], protein-small molecule [31] and protein-metal

ion complexes [32], as well as for other biological complexes, such as DNA duplexes [33-34]. However, to the best of our knowledge, absolute values of k_{on} and k_{off} for protein-ligand interactions measured using this approach have not been previously reported. Here, we describe the application ESI-MS for quantifying k_{off} for the high affinity interaction between biotin (B) and a truncated form (containing residues 13-139) of wild-type (WT) streptavidin. Streptavidin is a homotetrameric protein complex (S_4) that is isolated from *Streptomyces avidinii* [35]. Each streptavidin subunit is organized into an 8-stranded β-barrel, with a binding site for B at one end [36]. The streptavidin-biotin interaction is one of the most stable in nature and the exceptionally high affinity (K_a of ~2.5×10^{13} M^{-1} at pH 7.4 and 25 °C) arises from an unusually small dissociation rate constant (5.4×10^{-6} s^{-1} at pH 7.4 and 25 °C) [13]. The origin of the slow dissociation kinetics has been the focus of many experimental and theoretical studies [13-14,37-40]. For example, the temperature dependence of k_{off} for the interaction between B and WT streptavidin has been compared with values measured for a variety of single site mutants in an effort to elucidate the influence of the specific amino acid side chains on the kinetic barrier to dissociation [13-14,41]. These data were measured using a radiolabeled B assay, whereby the release of bound B from (S_4 + 4B) complex was monitored in the presence of an excess of unlabeled B. In the present study, values of k_{off} for the sequential loss of B from the (S_4 + 4B) complex, at pH 7 and temperatures ranging from 15 to 45 °C, were measured using ESI-MS. Two different approaches were used to analyze the ESI-MS data, one based on the initial rate of change in the relative abundance of the (S_4 + 4B) species, the other based on non-linear fitting of the time-dependent relative abundances of all free and B-bound S_4 species. The Arrhenius parameters determined from the k_{off} values measured by ESI-MS were compared to the values obtained using the radiolabeled B assay [14]. In addition to providing a quantitative measure of

the dissociation rate constants, the direct ESI-MS measurements provide a definitive answer to the question of whether the sequential binding of B to S_4 occurs in a cooperative or non-cooperative fashion.

Experimental Section

Streptavidin and biotin

The plasmid for natural core streptavidin (containing residues 13-139 of WT streptavidin, MW 13 271 Da) was a gift from Prof. P. Stayton (University of Washington). Streptavidin was expressed in *E. coli* and purified using procedures described elsewhere [42]. Solutions of purified S_4 were exchanged directly into 100 mM aqueous ammonium acetate buffer using an Amicon microconcentrator with a MW cut-off of 10 kDa and lyophilized. Stock solutions of S_4 (100 μM) were prepared by dissolving a known amount of lyophilized streptavidin into 100 mM ammonium acetate and stored at -20 °C until needed. Biotin (B, MW 244.3 Da) was purchased from Sigma-Aldrich Canada (Oakville, Canada). The stock solution of B (800 μM) was prepared by dissolving B in Milli-Q water. All stock solutions were stored at -20 °C until needed.

Mass spectrometry

All measurements were performed using an Apex Qe 9.4T Fourier-transform ion cyclotron resonance (FTICR) mass spectrometer (Bruker, Billerica, MA). Nanoflow ESI (nanoESI) was performed using borosilicate tubes (1.0 mm o.d., 0.68 mm i.d.), pulled to ~5 μm o.d. at one end using a P-97 micropipette puller (Sutter Instruments, Novato, CA). The electric field required to spray the solution in positive ion mode was established by applying a voltage of 1.0 – 1.3 kV to a platinum wire inserted inside the glass tip. The solution flow rate was typically ~20 nL min^{-1}.

Details of the instrumental and experimental conditions typically used for quantifying protein-ligand interactions can be found elsewhere [43].

Kinetic measurements

For the kinetic measurements, the reaction mixtures were prepared by mixing aliquots of the stock solutions to achieve the desired concentrations of S_4 (10 µM), B (10 - 26 µM) and ammonium acetate (5 mM). The reaction mixtures were kept at constant temperature (15 - 45 °C) using a water bath (Colora, Germany). Aliquots of the reaction mixtures were removed at specific reaction times (t) and analyzed by ESI-MS. Three ESI mass spectra were measured for each aliquot. An acquisition time of approximately 1 min was used for each mass spectrum.

Data analysis

Assuming that the four ligand binding sites of S_4 are kinetically equivalent and independent, *vide infra*, the apparent rate constants for ligand association and dissociation reactions ($k_{on,i}$ and $k_{off,(i+1)}$, respectively) for each (S_4 + iB) species (eq 1) are related to the intrinsic (microscopic) rate constants (k_{on} and k_{off}) through statistical factors, which reflect the number of free and occupied binding sites, eqs 2a and 2b:

$k_{on,i}$

$$(S_4 + iB) + B \rightleftarrows (S_4 + (i+1)B) \quad (1)$$

$k_{off,(i+1)}$

$$k_{on,i} = (4- i)k_{on} \quad (2a)$$

$$k_{off,(i+1)} = (i+1)k_{off} \quad (2b)$$

It follows that the rate of change of the concentration of each (S_4 + iB) species can be described by eqs 3a-3e:

$$\frac{d([S_4])}{dt} = -4k_{on}[B][S_4] + k_{off}[S_4 + B] \quad (3a)$$

$$\frac{d([S_4 + B])}{dt} = -(3k_{on}[B] + k_{off})[S_4 + B] + 4k_{on}[B][S_4] + 2k_{off}[S_4 + 2B] \quad (3b)$$

$$\frac{d([S_4 + 2B])}{dt} = -(2k_{on}[B] + 2k_{off})[S_4 + 2B] + 3k_{on}[B][S_4 + B] + 3k_{off}[S_4 + 3B] \quad (3c)$$

$$\frac{d([S_4 + 3B])}{dt} = -(k_{on}[B] + 3k_{off})[S_4 + 3B] + 2k_{on}[B][S_4 + 2B] + 4k_{off}[S_4 + 4B] \quad (3d)$$

$$\frac{d([S_4 + 4B])}{dt} = -4k_{off}[S_4 + 4B] + k_{on}[B][S_4 + 3B] \quad (3e)$$

where $[S_4 + iB]$ is the concentration of the (S_4 + iB) species and [B] is the concentration of free B.

Because the rate of association of B to S_4 is very high, [B] will be extremely small when sub-stoichiometric amounts of ligand are used (which is the case in the present study). Consequently, it is reasonable to assume that [B] exists at a steady-state over the course of the entire reaction. Therefore, the ik_{on}[B] terms can be approximated as ik_1, where k_1 is a pseudo first-order rate constant. Eqs 3a-3e can then be rewritten in terms of the normalized abundances ($A_{R(S_4+iB)}$) of the (S_4 + iB) species, eqs 4a-4e:

$$\frac{dA_{RS_4}}{dt} = -4k_1 A_{RS_4} + k_{off} A_{R(S_4+B)} \quad (4a)$$

$$\frac{dA_{R(S_4+B)}}{dt} = -(3k_1 + k_{off}) A_{R(S_4+B)} + 4k_1 A_{RS_4} + 2k_{off} A_{R(S_4+2B)} \quad (4b)$$

$$\frac{dA_{R(S_4+2B)}}{dt} = -(2k_1 + 2k_{off})A_{R(S_4+2B)} + 3k_1 A_{R(S_4+B)} + 3k_{off} A_{R(S_4+3B)} \quad (4c)$$

$$\frac{dA_{R(S_4+3B)}}{dt} = -(k_1 + 3k_{off})A_{R(S_4+3B)} + 2k_1 A_{R(S_4+2B)} + 4k_{off} A_{R(S_4+4B)} \quad (4d)$$

$$\frac{dA_{R(S_4+4B)}}{dt} = -4k_{off} A_{R(S_4+4B)} + k_1 A_{R(S_4+3B)} \quad (4e)$$

As described below, under the solution conditions used in the present study, there is a significant difference in the ligand association and dissociation rates immediately upon mixing S_4 and B. [9,13-14] Because of this and the fact that the initial concentration of B is less than the total concentration of binding sites, mixing S_4 with B initially produces a non-equilibrium distribution of (S_4 + *i*B), one that favours the S_4 and (S_4 + 4B) species. As the reaction proceeds, the relative abundance of (S_4 + 4B) will decrease and system will eventually achieve an equilibrium distribution of (S_4 + *i*B) species. Because $A_{R(S_4+3B)}$ is initially relatively small, the rate of change of $A_{R(S_4+4B)}$, described by eq 4e, can be approximated by eq 5:

$$\frac{dA_{R(S_4+4B)}}{dt} \approx -4k_{off} A_{R(S_4+4B)} \quad (5)$$

and k_{off} can be evaluated from a linear least squares fit of the plot of the natural logarithm of $A_{R(S_4+4B)}$ versus *t*, eq 6:

$$\ln A_{R(S_4+4B)} = -4k_{off} \times t + b \quad (6)$$

where b is a constant that is equal to $\ln A_{R(S_4+4B)}$ at t = 0. In this case, t = 0 corresponds to the earliest reaction time for which ESI mass spectra were acquired. It should be noted that the magnitude of b depends on the initial concentrations of S_4 and B.

An alternative approach to determining k_{off} involves applying non-linear regression analysis to the time-dependence of $A_{R(S_4+iB)}$ for each (S_4 + iB) species. This approach is more general than the initial rate method described above since there are no simplifying assumptions needed and k_1, in addition to k_{off}, can be determined. Moreover, this approach is not limited to data measured early in the reaction. In fact, inclusion of data measured at longer times, where the system is approaching equilibrium, enhances the reliability of the fitting procedure. Expressions for the time-dependent $A_{R(S_4+iB)}$ for each (S_4 + iB) species are obtained by solving eqs 4a-e (as a system) using Maple 14 (Maplesoft, Waterloo, Canada). The experimental $A_{R(S_4+iB)}$ values at t = 0 (the earliest time point measured) served as a boundary conditions. Shown in Supplementary Data is a set of solutions (functions) corresponding to experimental data acquired at 44.8 °C. Origin (OriginLab, Northampton, MA) was used to fit the functions (with k_{off} and k_1 as adjustable parameters) to the experimental breakdown curves ($A_{R(S_4+iB)}$ values plotted versus t). At each temperature, k_{off} and k_1 values were calculated for each (S_4 +iB) species; the reported k_{off} and k_1 values in Table 1 correspond to the average of these values.

The temperature dependence of the measured k_{off} values was analyzed according to the Arrhenius equation, eq 7:

$$\ln(k_{off}) = -\frac{E_a}{RT} + \ln(A) \qquad (7)$$

The activation energy (E_a) and pre-exponential factor (A) were calculated from the slope and intercept, respectively, of a linear least-squares fit of the plot of $\ln(k_{off})$ versus 1/T.

Results and discussion

Shown in Figures 1a to 1c are representative ESI mass spectra acquired in positive ion mode for a solution (pH 7 and 22.1 °C) of S_4 (10 μM) and B (14 μM) and ammonium acetate (5 mM) immediately after mixing (i.e., reaction time ~ 0 min), and after 112 min and 1602 min (1.1 days). In each mass spectrum, signals corresponding to the protonated $(S_4 + iB)^{n+}$ ions with $0 \leq i \leq 4$, at n = 12 – 16, are evident. Initially, the S_4^{n+} and $(S_4 + 4B)^{n+}$ ions represent the dominant species present (Figure 1a). The observation of predominantly free and fully ligand-bound protein shortly after mixing B with S_4 is consistent with results of Sano and Cantor [44]. These authors used gel electrophoresis to analyze solutions of B and S_4, immediately after mixing, and observed only two major bands, which corresponded to S_4 and $(S_4 + 4B)$. [44] The authors interpreted these results as evidence of cooperative ligand binding [44]. However, the observation of abundant S_4 and $(S_4 + 4B)$ in the ESI mass spectra does not necessarily imply cooperative binding of B to S_4. Instead, mixing of S_4 and B could lead initially to a non-equilibrium distribution of streptavidin-biotin species due to the fast association kinetics and extremely slow dissociation kinetics. The latter explanation finds support in the observation that the distribution of $(S_4 + iB)$ species changes at longer reaction times. For example, after 112 min, abundant signal is observed for all five of the $(S_4 + iB)$ species, i.e., with *i* from 0 to 4, although S_4 remains the dominant species detected (Figure 1b); after 1602 min, the $(S_4 + B)$ species dominates (Figure 1c). At much longer times, a constant distribution of $(S_4 + iB)$ species is observed, indicating that an equilibrium distribution of $(S_4 + iB)$ species was reached. As an example, shown in Figure 1d is a representative ESI mass spectrum acquired after 13080 min (9

days). Notably, the measured distribution of (S_4 + *i*B) species agrees with the distribution expected in the case of four identical and independent ligand binding sites, each with a microscopic K_a of 2.5×10^{13} M^{-1} (at pH 7.4 and 25 °C) (Figure 1e) [13]. These results establish, unambiguously, that B binding to S_4 is not a cooperative process, in agreement with the findings of Jones and Kurzban [45] and Fidelio and co-workers [46], and that the binding sites are thermodynamically equivalent and independent. It is also concluded that the apparent cooperative distributions of the (S_4 + *i*B) species observed at short reaction times are, in fact, of kinetic and not thermodynamic origin.

As noted in the Data Analysis section, two different approaches were used to quantify k_{off}. One approach is based on the initial rate of change of $A_{R(S_4+iB)}$. Shown in Figure 2a are plots of the natural logarithm of $A_{R(S_4+iB)}$ versus *t*, measured at the reaction temperatures indicated. Importantly, the plots exhibit excellent linearity. This result indicates that neglect of the ligand association reaction involving (S_4 + 3B) to $A_{R(S_4+4B)}$ in eq 4e is a reasonable assumption. The k_{off} values calculated at each reaction temperature are listed in Table 1. Notably, the value of 5.0×10^{-5} s^{-1} determined at 36.2 °C agrees very well with the reported value of 4.1×10^{-5} s^{-1}, which was measured at 37 °C [14]. An alternative approach used to determine k_{off} involves non-linear fitting of the solutions of eqs 4a-4e to the time-dependent $A_{R(S_4+iB)}$ values. Plotted in Figure 2b are the $A_{R(S_4+iB)}$ values measured at 44.8 °C and the curves obtained from the non-linear fitting procedure. It can be seen that the calculated curves describe the experimental data very well. The average kinetic parameters, determined at each temperature investigated, are summarized in Table 1. Notably, the k_{off} values determined by the two different methods agree very well, within a factor of 2, at all of the temperatures investigated. For example, a k_{off} value of 5.0×10^{-5} s^{-1} was

determined at 36.2°C with the non-linear fitting method, which is indistinguishable from the value of 5.1×10^{-5} s^{-1} determined from the initial rates approach. With the non-linear fitting method, the k_1 ($=k_{on}$[B]) terms were also established at each temperature investigated (Table 1). Although [B] is not accurately known (and, in fact, varies over the course of the reaction), it is nevertheless possible to estimate k_{on} by assuming that [B] (at all reaction times) is similar in magnitude to the $[B]_{eq}$, the concentration of free B at equilibrium. Following this approach, k_{on} was estimated to be 1.3×10^{8} $M^{-1}s^{-1}$ at 22.1°C using a $[B]_{eq}$ of 2.2×10^{-14} M, which was calculated for a solution of S_4 (10 μM) and B (14 μM) and a microscopic K_a of 2.5×10^{13} M^{-1} [13]. This value of k_{on} agrees reasonably well with a value of 4.5×10^{7} $M^{-1}s^{-1}$, which was determined from measurements carried out at ambient temperature (not specified) using droplet microfluidics integrated with a confocal fluorescence detection system [9].

Shown in Figure 3 are the Arrhenius plots constructed from the k_{off} values determined from the ESI-MS data using the two different data analysis approaches. The corresponding Arrhenius parameters (E_a, A) are listed in Table 2. Also shown in Figure 3 is the calculated curve based on the reported activation enthalpy and entropy, for the loss of B from the (S_4 + 4B) complex in aqueous solution at pH 7.4 [14]. Inspection of Figure 3 (and Table 2) reveals that the Arrhenius plots for the loss of B from the (S_4 + 4B) complex from linear and nonlinear fitting are similar, with E_a values of 30.4 ± 0.7 and 31.7 ± 0.8 kcal mol^{-1}, respectively. Moreover, the E_a values agree with the reported value of 31.0 ± 0.2 kcal mol^{-1} [14]. These findings indicate that both approaches to the analysis of the time-resolved ESI-MS data can provide a reliable determination of the temperature-dependence of k_{off}. However, the non-linear fitting approach is more general and, in principle, can be applied in cases where sequential ligand binding exhibits cooperativity or where multiple, non-equivalent binding sites are present.

The streptavidin-biotin interaction is unusually kinetically stable and it takes several days to achieve an equilibrium distribution of (S_4 + *i*B) species at the temperatures investigated. However, it is important to note that this same experimental approach could be applied, in an on-line fashion, to determine k_{off} and, in principle, k_{on} for protein-ligand interactions that require less time to reach an equilibrium distribution. Given that ~1 min is typically required to acquire an ESI mass spectrum (with a high signal-to-noise ratio) for solutions of protein-ligand complexes [44], it should be possible to apply this approach to complexes that take >10 min (under the desired solution conditions) to reach equilibrium. Although this approach will not be suitable for all protein-ligand complexes (those that exhibit both fast association and dissociation kinetics), the kinetic parameters for many protein-ligand interactions are expected to be accessible with this technique [48,49].

Conclusion

In summary, ESI-MS measurements have been used to quantify k_{off} for the sequential loss of B from the (S_4 + 4B) complex at pH 7 and temperatures ranging from 15 to 45 °C. Two different general strategies for data analysis were considered, one based on the initial rate of dissociation of the (S_4 + 4B) complex, and the other employing non-linear fitting of the time-dependent $A_{R(S_4+iB)}$ values of the (S_4 + *i*B) species. The two methods were found to yield k_{off} values that agree within a factor of two. Importantly, the dissociation E_a values measured by ESI-MS agree within 1 kcal mol^{-1} with the reported value, which was measured using a radiolabeled B assay. In addition to providing a quantitative measure of k_{off} at the temperatures investigated, the ESI-MS measurements also revealed, unambiguously, that sequential B binding to S_4 occurs in a non-cooperative fashion and that the four ligand binding sites are kinetically and thermodynamically equivalent and independent.

Acknowledgement

The authors are grateful for financial support provided by the Natural Sciences and Engineering Research Council of Canada and the Alberta Glycomics Centre. The authors acknowledge Professor P. Stayton (University of Washington) for generously providing the streptavidin plasmid.

References

1. Copeland, R.A., Pompliano, D.L., Meek, T.D.: Drug-target residence time and its implications for lead optimization. *Nat. Rev. Drug Discov.* **5,** 730-739 (2006)

2. Swinney, D.C.: The role of binding kinetics in therapeutically useful drug action. *Curr. Opin. Drug Discovery Dev.* **12,** 31-39 (2009)

3. Callender, R., Dyer, R.B.: Advances in Time-Resolved Approaches To Characterize the Dynamical Nature of Enzymatic Catalysis. *Chem. Rev.* **106,** 3031-3042 (2006)

4. Daghestani, H.N., Day, B.W.: Theory and Applications of Surface Plasmon Resonance, Resonant Mirror, Resonant Waveguide Grating, and Dual Polarization Interferometry Biosensors. *Sensors* **10,** 9630-9646 (2010)

5. De Crescenzo, G., Boucher, C., Durocher, Y., Jolicoeur, M.: Kinetic Characterization by Surface Plasmon Resonance-Based Biosensors: Principle and Emerging Trends. *Cell. Mol. Bioeng.* **1,** 204-215 (2008)

6. Bizzarri, A.R., Cannistraro, S.: Atomic Force Spectroscopy in Biological Complex Formation: Strategies and Perspectives. *J. Phy. Chem. B* **113,** 16449-16464 (2009)

7. Hill, J.J., Royer, C.A.: Fluorescence approaches to study of protein-nucleic acid complexation. *Methods Enzymol.* **278,** 390-416 (1997)

8. Málnási-Csizmadia, A., Pearson, D.S., Kovács, M., Woolley, R.J., Geeves, M.A., Bagshaw, C.R.: Kinetic Resolution of a Conformational Transition and the ATP Hydrolysis Step Using Relaxation Methods with a Dictyostelium Myosin II Mutant Containing a Single Tryptophan Residue. *Biochemistry* **40,** 12727-12737 (2001)

9. Srisa-Art, M., Dyson, E.C., deMello, A.J., Edel, J.B.: Monitoring of Real-Time Streptavidin−Biotin Binding Kinetics Using Droplet Microfluidics. *Anal. Chem.* **80,** 7063-7067 (2008)

10. Sugawara, T., Kuwajima, K., Sugai, S.: Folding of staphylococcal nuclease A studied by equilibrium and kinetic circular dichroism spectra. *Biochemistry* **30,** 2698-2706 (1991)

11. Chu, Y.H., Cheng, C.C.: Affinity capillary electrophoresis in biomolecular recognition. *Cell. Mol. Life Sci.* **54,** 663-683 (1998)

12. Hall, D.R., Winzor, D.J.: Potential of biosensor technology for the characterization of interactions by quantitative affinity chromatography. *J. Chromatogr. B* **715,** 163-181 (1998)

13. Chilkoti, A., Stayton, P.S.: Molecular Origins of the Slow Streptavidin-Biotin Dissociation Kinetics. *J. Am. Chem. Soc.* **117,** 10622-10628 (1995)

14. Klumb, L.A., Chu, V., Stayton, P.S.: Energetic Roles of Hydrogen Bonds at the Ureido Oxygen Binding Pocket in the Streptavidin−Biotin Complex. *Biochemistry* **37,** 7657-7663 (1998)

15. Gizachew, D., Dratz, E.: Transferred NOESY NMR Studies of Biotin Mimetic Peptide (FSHPQNT) Bound to Streptavidin: A Structural Model for Studies of Peptide–Protein Interactions. *Chem. Biol. Drug Des.* **78,** 14-24 (2011)

16. Bao, J., Krylova, S.M., Wilson, D.J., Reinstein, O., Johnson, P.E., Krylov, S.N.: Kinetic Capillary Electrophoresis with Mass-Spectrometry Detection (KCE-MS) Facilitates Label-Free Solution-Based Kinetic Analysis of Protein–Small Molecule Binding. *ChemBioChem* **12,** 2551-2554 (2011)

17. Konermann, L., Collings, B.A., Douglas, D.J.: Cytochrome c Folding Kinetics Studied by Time-Resolved Electrospray Ionization Mass Spectrometry. *Biochemistry* **36,** 5554-5559 (1997)

18. Lee, V.W.S., Chen, Y.-L., Konermann, L.: Reconstitution of Acid-Denatured Holomyoglobin Studied by Time-Resolved Electrospray Ionization Mass Spectrometry. *Anal. Chem.* **71,** 4154-4159 (1999)

19. Sobott, F., Benesch, J.L.P., Vierling, E., Robinson, C.V.: Subunit exchange of multimeric protein complexes. Real-time monitoring of subunit exchange between small heat shock proteins by using electrospray mass spectrometry. *J. Biol. Chem.* **277,** 38921-38929 (2002)

20. Simmons, D.A., Wilson, D.J., Lajoie, G.A., Doherty-Kirby, A., Konermann, L.: Subunit Disassembly and Unfolding Kinetics of Hemoglobin Studied by Time-Resolved Electrospray Mass Spectrometry. *Biochemistry* **43,** 14792-14801 (2004)

21. Deng, G., Sanyal, G.: Applications of mass spectrometry in early stages of target based drug discovery. *J. Pharm. Biomed. Anal.* **40,** 528-538 (2006)

22. Pan, J., Rintala-Dempsey, A.C., Li, Y., Shaw, G.S., Konermann, L.: Folding Kinetics of the S100A11 Protein Dimer Studied by Time-Resolved Electrospray Mass Spectrometry and Pulsed Hydrogen−Deuterium Exchange. *Biochemistry* **45,** 3005-3013 (2006)

23. Sharon, M., Robinson, C.V.: The Role of Mass Spectrometry in Structure Elucidation of Dynamic Protein Complexes. *Annu. Rev. Biochem* **76,** 167-193 (2007)

24. Clarke, D.J., Stokes, A.A., Langridge-Smith, P., Mackay, C.L.: Online Quench-Flow Electrospray Ionization Fourier Transform Ion Cyclotron Resonance Mass Spectrometry for Elucidating Kinetic and Chemical Enzymatic Reaction Mechanisms. *Anal. Chem.* **82,** 1897-1904 (2010)

25. Robbins, M.D., Yoon, O.K., Barbula, G.K., Zare, R.N.: Stopped-Flow Kinetic Analysis Using Hadamard Transform Time-of-Flight Mass Spectrometry. *Anal. Chem.* **82,** 8650-8657 (2010)

26. Miao, Z., Chen, H., Liu, P., Liu, Y.: Development of Submillisecond Time-Resolved Mass Spectrometry Using Desorption Electrospray Ionization. *Anal. Chem.* **83,** 3994-3997 (2011)

27. Pacholarz, K.J., Garlish, R.A., Taylor, R.J., Barran, P.E.: Mass spectrometry based tools to investigate protein-ligand interactions for drug discovery. *Chem. Soc. Rev.* **41,** 4335-4355 (2012)

28. Goodlett, D.R., Ogorzalek Loo, R.R., Loo, J.A., Wahl, J.H., Udseth, H.R., Smith, R.D.: A study of the thermal denaturation of ribonuclease S by electrospray ionization mass spectrometry. *J. Am. Soc. Mass. Spectrom.* **5,** 614-622 (1994)

29. Soya, N., Fang, Y., Palcic, M.M., Klassen, J.S.: Trapping and characterization of covalent intermediates of mutant retaining glycosyltransferases. *Glycobiology* **21,** 547-552 (2011)

30. Deroo, S., Hyung, S.-J., Marcoux, J., Gordiyenko, Y., Koripella, R.K., Sanyal, S., Robinson, C.V.: Mechanism and Rates of Exchange of L7/L12 between Ribosomes and the Effects of Binding EF-G. *ACS Chem. Biol.* **7,** 1120-1127 (2012)

31. Peleg-Shulman, T., Najajreh, Y., Gibson, D.: Interactions of cisplatin and transplatin with proteins: Comparison of binding kinetics, binding sites and reactivity of the Pt-protein adducts of cisplatin and transplatin towards biological nucleophiles. *J. Inorg. Biochem.* **91,** 306-311 (2002)

32. Pan, J., Konermann, L.: Calcium-Induced Structural Transitions of the Calmodulin−Melittin System Studied by Electrospray Mass Spectrometry: Conformational Subpopulations and Metal-Unsaturated Intermediates. *Biochemistry* **49,** 3477-3486 (2010)

33. Rosu, F., Gabelica, V., Shin-ya, K., De Pauw, E.: Telomestatin-induced stabilization of the human telomeric DNA quadruplex monitored by electrospray mass spectrometry. *Chem. Commun.* 2702-2703 (2003)

34. Gabelica, V., Rosu, F., De Pauw, E.: A Simple Method to Determine Electrospray Response Factors of Noncovalent Complexes. *Anal. Chem.* **81,** 6708-6715 (2009)

35. L. Chaiet, F.J.W.: The properties of streptavidin, a biotin-binding protein produced by Streptomycetes. *Arch. Biochem. Biophys.* **106,** 1-5 (1964)

36. Hendrickson, W.A., Pähler, A., Smith, J.L., Satow, Y., Merritt, E.A., Phizackerley, R.P.: Crystal structure of core streptavidin determined from multiwavelength anomalous diffraction of synchrotron radiation. *Proc. Natl. Acad. Sci. U.S.A.* **86,** 2190-2194 (1989)

37. Chu, V., Stayton, P.S., Freitag, S., Le Trong, I., Stenkamp, R.E.: Thermodynamic and structural consequences of flexible loop deletion by circular permutation in the streptavidin-biotin system. *Protein Sci.* **7,** 848-859 (1998)

38. Stayton, P.S., Freitag, S., Klumb, L.A., Chilkoti, A., Chu, V., Penzotti, J.E., To, R., Hyre, D., Le Trong, I., Lybrand, T.P., Stenkamp, R.E.: Streptavidin–biotin binding energetics. *Biomol. Eng* **16,** 39-44 (1999)

39. Li, Q., Gusarov, S., Evoy, S., Kovalenko, A.: Electronic Structure, Binding Energy, and Solvation Structure of the Streptavidin−Biotin Supramolecular Complex: ONIOM and 3D-RISM Study. *J. Phy. Chem. B* **113,** 9958-9967 (2009)

40. Deng, L., Broom, A., Kitova, E.N., Richards, M.R., Zheng, R.B., Shoemaker, G.K., Meiering, E.M., Klassen, J.S.: Kinetic Stability of the Streptavidin–Biotin Interaction Enhanced in the Gas Phase. *J. Am. Chem. Soc.* **134,** 16586-16596 (2012)

41. Piran, U., Riordan, W.J.: Dissociation rate constant of the biotin-streptavidin complex. *J. Immunol. Methods* **133,** 141-143 (1990)

42. Chilkoti, A., Tan, P.H., Stayton, P.S.: Site-directed mutagenesis studies of the high-affinity streptavidin-biotin complex: contributions of tryptophan residues 79, 108, and 120. *Proceedings of the National Academy of Sciences* **92,** 1754-1758 (1995)

43. El-Hawiet, A., Kitova, E.N., Kitov, P.I., Eugenio, L., Ng, K.K., Mulvey, G.L., Dingle, T.C., Szpacenko, A., Armstrong, G.D., Klassen, J.S.: Binding of Clostridium difficile toxins to human milk oligosaccharides. *Glycobiology* **21,** 1217-1227 (2011)

44. Kitova, E., El-Hawiet, A., Schnier, P., Klassen, J.: Reliable Determinations of Protein–Ligand Interactions by Direct ESI-MS Measurements. Are We There Yet? *J. Am. Soc. Mass. Spectrom.* **23,** 431-441 (2012)

45. Sano, T., Cantor, C.R.: Cooperative biotin binding by streptavidin. Electrophoretic behavior and subunit association of streptavidin in the presence of 6 M urea. *J. Biol. Chem.* **265,** 3369-3373 (1990)

46. Jones, M.L., Kurzban, G.P.: Noncooperativity of Biotin Binding to Tetrameric Streptavidin. *Biochemistry* **34,** 11750-11756 (1995)

47. Gonzalez, M., Bagatolli, L., Echabe, I., Arrondo, J., Argarana, C., Cantor, C., Fidelio, G.: Interaction of biotin with streptavidin - Thermostability and conformational changes upon binding *J. Biol. Chem.* **272,** 11288-11294 (1997)

48. Nunez, S., Venhorst, J., Kruse, C.G.: Target-drug interactions: first principles and their application to drug discovery. *Drug Discovery Today* **17,** 10-22 (2012)

49. Tummino, P.J., Copeland, R.A.: Residence Time of Receptor-Ligand Complexes and Its Effect on Biological Function. *Biochemistry* **47**, 5481-5492 (2008)

Table 1. Microscopic rate constants (k_{off}) for the dissociation of the streptavidin-biotin interaction at pH 7 and temperatures ranging from 15 to 45 °C measured using direct ESI-MS analysis.[a,b]

$[S_4]_o$ (μM)	$[B]_o$ (μM)	T (°C)	k_{off} (s^{-1}) [a] Linear fitting	k_{off} (s^{-1}) [b] Non-linear fitting	k_1 (s^{-1}) [b] Non-linear fitting
10	20	15.3	$(1.1 \pm 0.1)\times10^{-6}$	$(1.3 \pm 0.7)\times10^{-6}$	$(2.3 \pm 0.8)\times10^{-6}$
10	14	22.1	$(4.1 \pm 0.1)\times10^{-6}$	$(5.5 \pm 0.3)\times10^{-6}$	$(2.8 \pm 0.9)\times10^{-6}$
10	10	30.5	$(1.8 \pm 0.1)\times10^{-5}$	$(2.1 \pm 0.1)\times10^{-5}$	$(8.7 \pm 0.3)\times10^{-6}$
10	10	36.2	$(5.0 \pm 0.2)\times10^{-5}$	$(5.1 \pm 0.1)\times10^{-5}$	$(1.8 \pm 0.3)\times10^{-5}$
10	10	44.8	$(1.6 \pm 0.1)\times10^{-4}$	$(2.5 \pm 0.2)\times10^{-4}$	$(8.4 \pm 0.7)\times10^{-5}$

a. k_{off} was obtained from the slope (k_{off} = ¼ slope) of a linear least squares fit of the plot of the natural logarithm of $A_{R(S_4+4B)}$ versus *t*. Reported errors correspond to one standard deviation. b. At each temperature, k_{off} and k_1 was obtained from non-linear regression analysis of the time-dependent relative abundance of each of the (S_4 + *i*B) species. The reported k_{off} and k_1 values correspond to the average of these values and errors are one standard deviation.

Table 2. Arrhenius activation parameters (E_a, A) for the loss of B from the (S_4 + 4B) complex determined from k_{off} values measured by ESI-MS (using linear and non-linear data analysis methods) at pH 7, and Arrhenius parameters measured at pH 7.4 using a radiolabeled biotin assay.

	E_a (kcal mol^{-1})	A (s^{-1})
ESI-MS (linear fitting)	30.4 ± 0.7 [a]	$10^{17.1 \pm 0.5}$ [a]
ESI-MS (non-linear fitting)	31.7 ± 0.8 [a]	$10^{18.2 \pm 0.6}$ [a]
Radiolabeled biotin assay	31.0 ± 0.2 [b]	$10^{17.3 \pm 0.1}$ [b]

Reported errors correspond to one standard deviation. b. Values calculated from the activation enthalpy and entropy reported in [14].

Figure captions

Figure 1. ESI mass spectra acquired for an aqueous ammonium acetate (5 mM) solution of S_4 (10 μM) and B (14 μM) at 22.1 °C and pH 7 and different reaction times (a) 0 sec (b) 112 min, (c) 1602 min (1.1 days) and (d) 13080 min (9 days). (e) Normalized distribution of (S_4 + *i* B) species, where *i* = 0 – 4, determined from the ESI mass spectrum shown in (d). The reported errors correspond to one standard deviation and were determined from 3 replicate measurements. Also shown is the calculated distribution for four equivalent ligand binding sites, each with a K_a of 2.5×10^{13} M^{-1}.

Figure 2. (a) Plots of the natural logarithm of $A_{R(S_4+4B)}$ versus reaction time measured by ESI-MS for neutral aqueous ammonium acetate (5 mM) solutions of S_4 (10 μM) and B (10 - 20 μM) at 15.3 °C, 22.1 °C, 30.5 °C, 36.2 °C and 44.8 °C. The solid curves represent linear least squares fits of the experimental data. (b) Plots of $A_{R(S_4+iB)}$ versus reaction time measured by ESI-MS neutral aqueous ammonium acetate (5 mM) solution of S_4 (10 μM), B (10 μM) at 44.8 °C. The solid curves were determined from non-linear regression analysis to the time-dependent $A_{R(S_4+iB)}$ values.

Figure 3. Arrhenius plots the loss of B from the (S_4 + 4B) complex at pH 7 constructed from k_{off} values measured by ESI-MS (linear fitting (▲), non-linear fitting (●)) and corresponding plot (- - -) calculated from the activation enthalpy and entropy reported in [14].

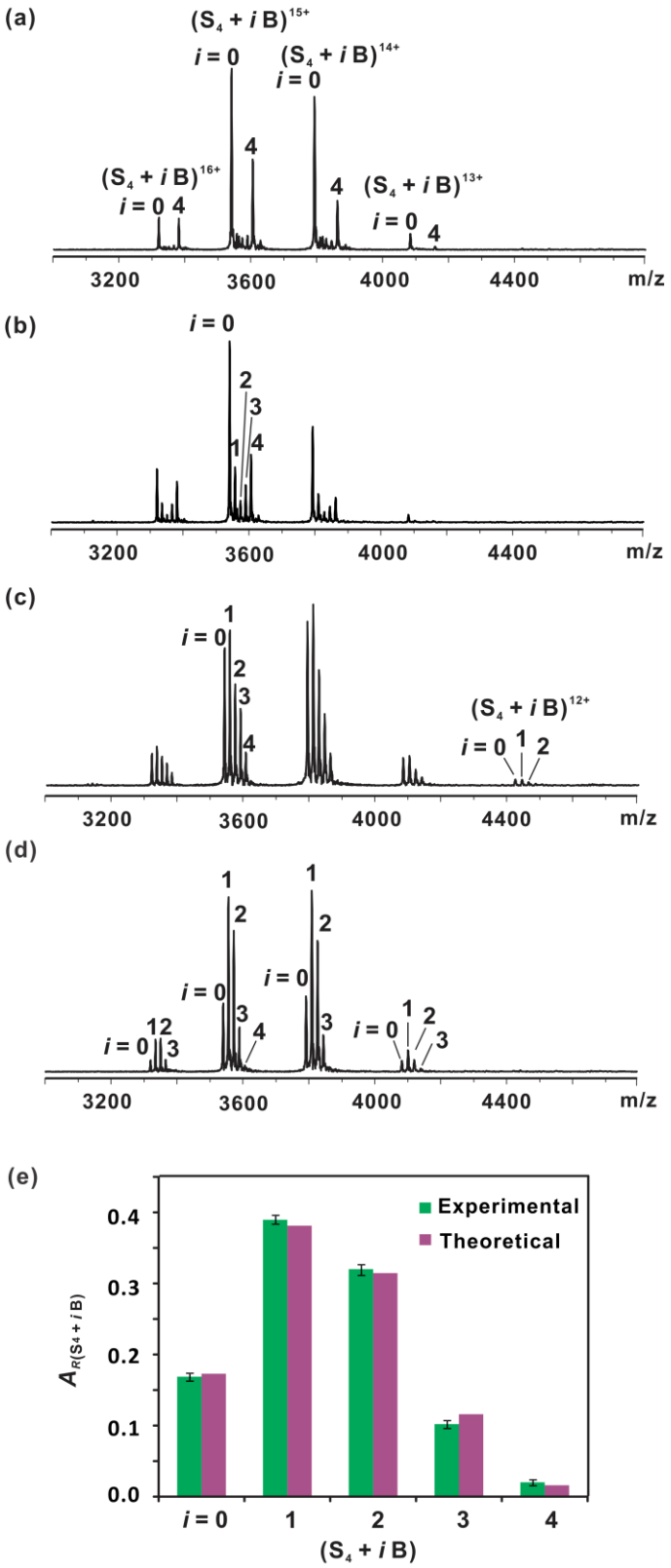
(a)
(S4 + i B)15+
i = 0
(S4 + i B)14+
i = 0
4
(S4 + i B)16+
i = 0 4
4
(S4 + i B)13+
i = 0
4
3200
3600
4000
4400
m/z
(b)
i = 0
2
3
1
4
3200
3600
4000
4400
m/z
(c)
1
i = 0
2
3
4
(S4 + i B)12+
i = 0 1 2
3200
3600
4000
4400
m/z
(d)
1
2
i = 0
3
4
1
2
i = 0
3
i = 0
12
3
1 2
3
3200
3600
4000
4400
m/z
(e)
Experimental
Theoretical
0.4
0.3
0.2
0.1
0.0
AR(S4 + i B)
i = 0
1
2
3
4
(S4 + i B)

Figure 1

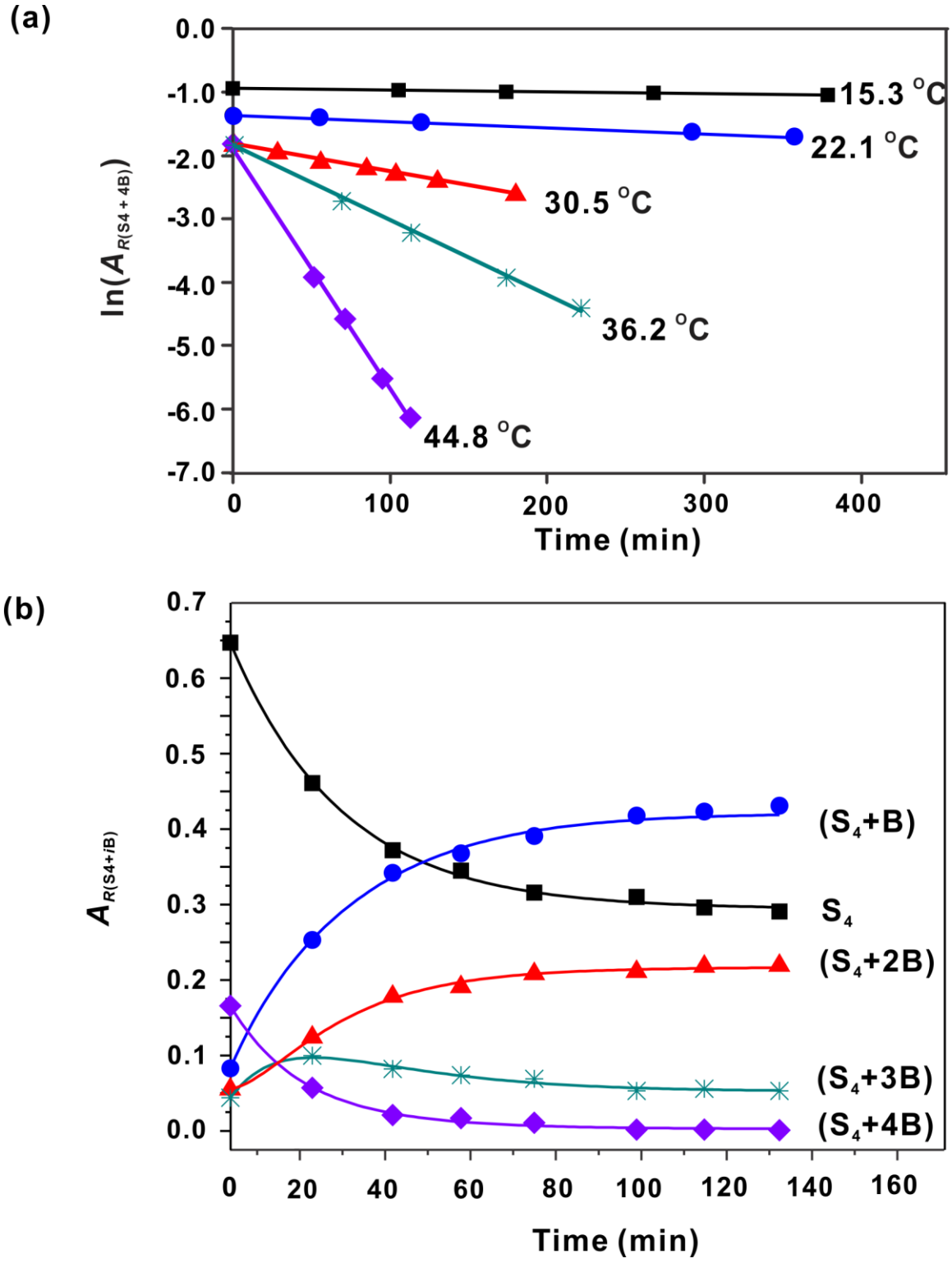
(a)
0.0
-1.0
-2.0
-3.0
-4.0
-5.0
-6.0
-7.0
ln(A R(S4 + 4B))
15.3 °C
22.1 °C
30.5 °C
36.2 °C
44.8 °C
0
100
200
300
400
Time (min)
(b)
0.7
0.6
0.5
0.4
0.3
0.2
0.1
0.0
A R(S4+iB)
(S4+B)
S4
(S4+2B)
(S4+3B)
(S4+4B)
0
20
40
60
80
100
120
140
160
Time (min)

Figure 2

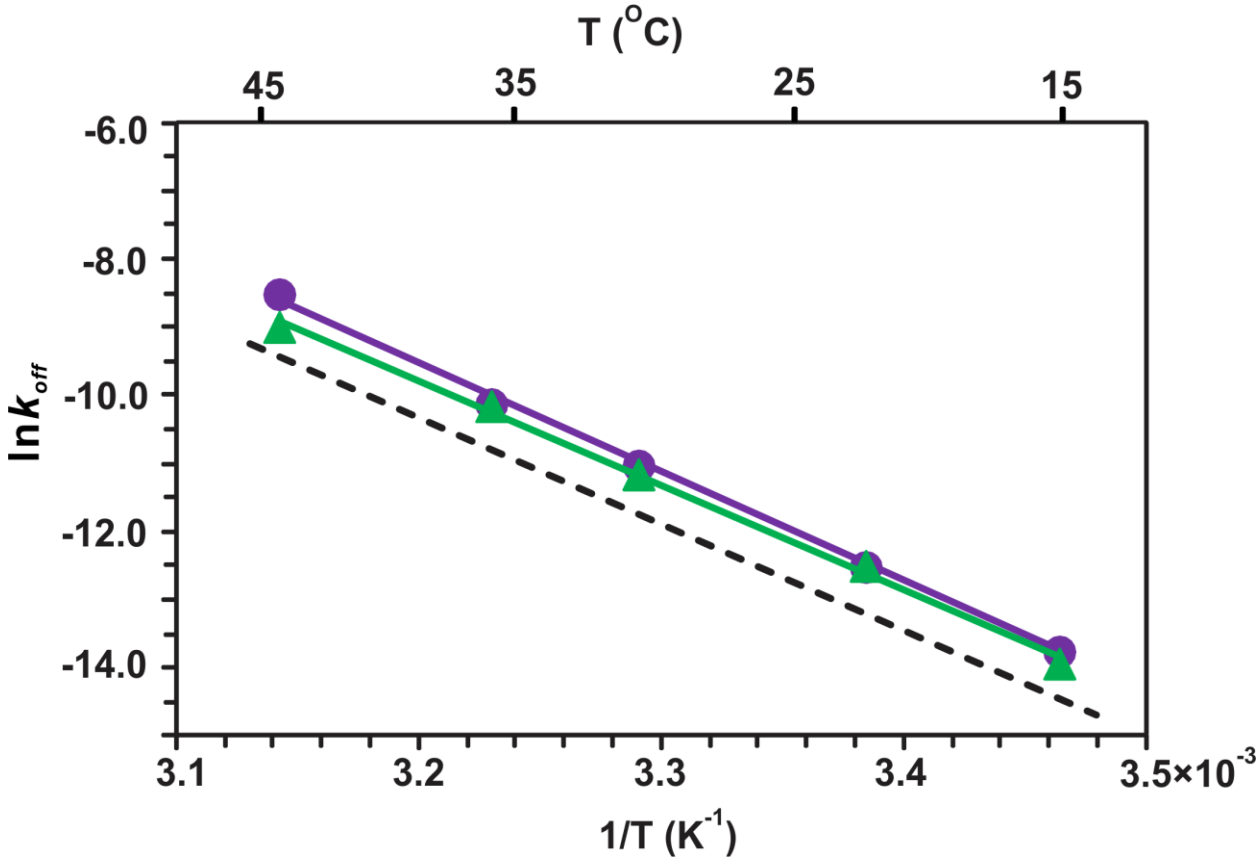

Figure 3

Supporting Information

Dissociation Kinetics of the Streptavidin-Biotin Interaction Measured using Direct Electrospray Ionization Mass Spectrometry Analysis

Lu Deng, Elena N. Kitova, and John S. Klassen*

Department of Chemistry and Alberta Glycomics Centre, University of Alberta, Edmonton, Alberta, Canada T6G 2G2

* Email: john.klassen@ualberta.ca

Sample solutions for the time dependence of the relative abundances of the (S_4 + *i*B) species

The following expressions for the time-dependent relative abundances of each of the (S_4 + *i*B) species ($A_{R(S_4+iB)}$) were obtained by solving eqs 4a-e (as a system) using Maple 14 (Maplesoft, Waterloo, Canada). The experimental values of $A_{R(S_4+iB)}$ at t = 0 (the earliest time point measured) acquired at 44.8 °C were applied as boundary conditions: A_{RS_4} = 0.648, $A_{R(S_4+B)}$ = 0.084, $A_{R(S_4+2B)}$ = 0.056, $A_{R(S_4+3B)}$ = 0.045, $A_{R(S_4+4B)}$ = 0.167.

$$A_{RS_4}(t) = k_{off}^4/(k_1^2+2k_{off}\times k_1+k_{off}^2)^2+(1/1000)\times(3001k_1-999k_{off})\times k_{off}^3\times\exp(-(k_1+k_{off})\times t)/(k_1^2+2k_{off}\times k_1+k_{off}^2)^2+(1/1000)\times(2676k_1^3-364k_{off}\times k_1^2+247k_{off}^2\times k_1-713k_{off}^3)\times k_{off}\times\exp(-3(k_1+k_{off})\times t)/((k_1^3+3k_{off}\times k_1^2+3k_{off}^2\times k_1+k_{off}^3)\times(k_1+k_{off}))+(1/1000)\times(167k_{off}^4+648k_1^4+56k_{off}^2\times k_1^2-84k_{off}\times k_1^3-45k_{off}^3\times k_1)\times\exp(-(4(k_1+k_{off})\times t)/(6k_{off}^2\times k_1^2+4k_{off}^3\times k_1+k_1^4+4k_{off}\times k_1^3+k_{off}^4)+(1/1000)\times(4196k_1^2-611k_{off}\times k_1+1193k_{off}^2)\times k_{off}^2\times\exp(-(2(k_1+k_{off})\times t)/(k_1^2+2k_{off}\times k_1+k_{off}^2)^2$$

$$A_{R(S_4+B)}(t) = ((3/1000)\times(3001k_1-999k_{off})\times k_{off}^3\times\exp(-(k_1+k_{off})\times t)\times k_1/(k_1^2+2k_{off}\times k_1+k_{off}^2)^2-(1/1000)\times(3001k_1-999k_{off})\times k_{off}^4\times\exp(-(k_1+k_{off})\times t)/(k_1^2+2k_{off}\times k_1+k_{off}^2)^2+(1/1000)\times(2676k_1^3-364k_{off}\times k_1^2+247k_{off}^2\times k_1-713k_{off}^3)\times k_{off}\times\exp(-(3(k_1+k_{off})\times t)\times k_1/((k_1^3+3k_{off}\times k_1^2+3k_{off}^2\times k_1+k_{off}^3)\times(k_1+k_{off}))-(3/1000)\times(2676k_1^3-364k_{off}\times k_1^2+247k_{off}^2\times k_1-713k_{off}^3)\times k_{off}^2\times\exp(-(3(k_1+k_{off})\times t)/((k_1^3+3k_{off}\times k_1^2+3k_{off}^2\times k_1+k_{off}^3)\times(k_1+k_{off}))-(1/250)\times(167k_{off}^4+648k_1^4+56k_{off}^2\times k_1^2-84k_{off}\times k_1^3-45k_{off}^3\times k_1)\times\exp(-(4(k_1+k_{off})\times t)\times k_{off}/(6k_{off}^2\times k_1^2+4k_{off}^3\times k_1+k_1^4+4k_{off}\times k_1^3+k_{off}^4)-(1/500)\times(4196k_1^2-611k_{off}\times k_1+1193k_{off}^2)\times k_{off}^3\times\exp(-2(k_1+k_{off})\times t)/(k_1^2+2k_{off}\times k_1+k_{off}^2)^2+(1/500)\times(4196k_1^2-611k_{off}\times k_1+1193k_{off}^2)\times k_{off}^2\times\exp(-2(k_1+k_{off})\times t)\times k_1/(k_1^2+2k_{off}\times k_1+k_{off}^2)^2+4k_1\times k_{off}^4/(k_1^2+2k_{off}\times k_1+k_{off}^2)^2)/k_{off}$$

$$A_{R(S_4+2B)}(t) = ((3/1000)\times k_1^2\times(3001k_1-999k_{off})\times k_{off}^3\times\exp(-(k_1+k_{off})\times t)/(k_1^2+2k_{off}\times k_1+k_{off}^2)^2+(1/1000)\times k_1^2\times(4196k_1^2-611k_{off}\times k_1+1193k_{off}^2)\times k_{off}^2\times\exp(-(2(k_1+k_{off})\times t)/(k_1^2+2k_{off}\times k_1+k_{off}^2)^2+(3/1000)\times(2676k_1^3-364k_{off}\times k_1^2+247k_{off}^2\times k_1-713k_{off}^3)\times k_{off}^3\times\exp(-(3(k_1+k_{off})\times t)/((k_1^3+3k_{off}k_1^2+3k_{off}^2\times k_1+k_{off}^3)\times(k_1+k_{off}))+(3/500)\times(167k_{off}^4+648k_1^4+56k_{off}^2\times k_1^2-84k_{off}\times k_1^3-45k_{off}^3\times k_1)\times\exp(-4(k_1+k_{off})\times t)\times k_{off}^2/(6k_{off}^2k_1^2+4k_{off}^3\times k_1+k_1^4+4k_{off}\times k_1^3+k_{off}^4)+(1/1000)\times(4196k_1^2-611k_{off}\times k_1+1193k_{off}^2)\times k_{off}^4\times\exp(-2(k_1+k_{off})\times t)/(k_1^2+2k_{off}\times k_1+k_{off}^2)^2+6k_1^2\times k_{off}^4/(k_1^2+2k_{off}\times k_1+k_{off}^2)^2-(3/1000)\times(3001k_1-999k_{off})\times k_{off}^4\times\exp(-(k_1+k_{off})\times t)\times k_1/(k_1^2+2k_{off}\times k_1+k_{off}^2)^2-(3/1000)\times(2676k_1^3-364k_{off}\times k_1^2+247k_{off}^2\times k_1-713k_{off}^3)\times k_{off}^2\times\exp(-$$

$3(k_1+k_{off})\times t)\times k_1/((k_1^3+3k_{off}\times k_1^2+3k_{off}^2\times k_1+k_{off}^3)\times(k_1+k_{off}))-(1/250)\times(4196k_1^2-611k_{off}\times k_1+1193k_{off}^2)\times k_{off}^3\times\exp(-2(k_1+k_{off})\times t\times k_1/(k_1^2+2k_{off}\times k_1+k_{off}^2)^2)/k_{off}^2$

$A_{R(S_4+3B)}(t) = -(-4k_1^3\times k_{off}^4/(k_1^2+2k_{off}\times k_1+k_{off}^2)^2-(1/1000)\times(3001k_1-999\times k_{off})\times k_{off}^3\times\exp(-(k_1+k_{off})\times t)\times k_1^3/(k_1^2+2k_{off}\times k_1+k_{off}^2)^2+(1/1000)\times(2676k_1^3-364k_{off}\times k_1^2+247k_{off}^2\times k_1-713k_{off}^3)\times k_{off}^4\times\exp(-(3(k_1+k_{off})\times t)/((k_1^3+3k_{off}\times k_1^2+3k_{off}^2\times k_1+k_{off}^3)\times(k_1+k_{off}))+(1/250)\times(167k_{off}^4+648k_1^4+56k_{off}^2\times k_1^2-84k_{off}\times k_1^3-45k_{off}^3\times k_1)\times\exp(-(4(k_1+k_{off})\times t)\times k_{off}^3/(6k_{off}^2\times k_1^2+4k_{off}^3\times k_1+k_1^4+4k_{off}\times k_1^3+k_{off}^4)+(3/1000)\times k_1^2\times(3001k_1-999k_{off})\times k_{off}^4\times\exp(-(k_1+k_{off})\times t)/(k_1^2+2k_{off}\times k_1+k_{off}^2)^2-(3/1000)\times(2676k_1^3-364k_{off}\times k_1^2+247k_{off}^2\times k_1-713k_{off}^3)\times k_{off}^3\times\exp(-(3(k_1+k_{off})\times t)\times k_1/((k_1^3+3k_{off}\times k_1^2+3k_{off}^2\times k_1+k_{off}^3)\times(k_1+k_{off}))-(1/500)\times(4196k_1^2-611k_{off}\times k_1+1193k_{off}^2)\times k_{off}^4\times\exp(-(2(k_1+k_{off})\times t)\times k_1/(k_1^2+2k_{off}\times k_1+k_{off}^2)^2+(1/500)\times k_1^2\times(4196k_1^2-611k_{off}\times k_1+1193k_{off}^2)\times k_{off}^3\times\exp(-2(k_1+k_{off})\times t)/(k_1^2+2k_{off}\times k_1+k_{off}^2)^2)/k_{off}^3$

$A_{R(S_4+4B)}(t) = (k_1^4\times k_{off}^4/(k_1^2+2k_{off}\times k_1+k_{off}^2)^2+(1/1000)\times(167k_{off}^4+648k_1^4+56k_{off}^2\times k_1^2-84k_{off}\times k_1^3-45k_{off}^3\times k_1)\times\exp(-(4(k_1+k_{off})\times t)\times k_{off}^4/(6k_{off}^2\times k_1^2+4k_{off}^3\times k_1+k_1^4+4k_{off}\times k_1^3+k_{off}^4)-(1/1000)\times(3001k_1-999k_{off})\times k_{off}^4\times\exp(-(k_1+k_{off})\times t)\times k_1^3/(k_1^2+2k_{off}\times k_1+k_{off}^2)^2-(1/1000)\times(2676k_1^3-364k_{off}\times k_1^2+247k_{off}^2\times k_1-713k_{off}^3)\times k_{off}^4\times\exp(-(3(k_1+k_{off})\times t)\times k_1/((k_1^3+3k_{off}\times k_1^2+3k_{off}^2\times k_1+k_{off}^3)\times(k_1+k_{off}))+(1/1000)\times k_1^2\times(4196k_1^2-611k_{off}\times k_1+1193k_{off}^2)\times k_{off}^4\times\exp(-(2(k_1+k_{of})\times t)/(k_1^2+2k_{off}\times k_1+k_{off}^2)^2)/k_{off}^4$